Neural Network Equalisation and Symbol Detection for 802.11p V2V Communication at 5.9GHz

Scott Stainton[†], Waseem Ozan[§], Martin Johnston[†], Satnam Dlay[†], and Paul Anthony Haigh[†]
[†]Intelligent Sensing & Communications Group, School of Engineering, Newcastle University, NE1 7RU, UK
[§]Information and Communications Engineering Group, University College London, WC1E 6BT, UK
email: {s.stainton2; martin.johnston; satnam.dlay; paul.haigh;}@newcastle.ac.uk,
w.ozan@ucl.ac.uk

***Abstract*—Neural networks are shown to be a viable implementation for joint channel equalisation and symbol detection in a vehicular network. Experimental results using a hardware-in-the-loop approach at 5.9GHz validate the efficacy of the proposed implementation following the 802.11p parameters using orthogonal frequency division multiplexing (OFDM). Further results are obtained using a more spectrally efficient waveform, namely spectrally efficient frequency division multiplexing (SEFDM), to show a trade-off between loss of orthogonality, and therefore bit-error rate (BER) performance, versus increased spectral efficiency to enable higher data rates or the ability to service more users. SEFDM is tested with compression factors ranging from 20% up to 60% bandwidth compression. The results show the neural network is able to achieve an acceptable BER performance in a highway non-line-of-sight (NLOS) channel which is a well established harsh and dynamic vehicular channel. This is further validated via measurements of the error vector magnitude.**

***Index Terms*—Machine Learning, OFDM, SEFDM, V2V**

I. Introduction

Vehicular communication, specifically vehicle-to-vehicle (V2V) communication, faces many challenges that differentiate it from more classic communication systems. One of these challenges is the harshness of the communication channel. Both the transmitter and receiver are at a similar height, which causes multiple reflections from surroundings that have slight path length differences, causing fast fading [1], [2]. This is exacerbated by Doppler effects due to the relative motion between the vehicles and the fact that the network topology is changing rapidly [3].

There have been several proposals to overcome these issues in the literature, one of which is the use of free space optics. In [4], the authors propose the use of lasers to achieve high speed communication over several hundred metres. One problem with this however is that line-of-sight (LOS) is required between devices which cannot be guaranteed in a vehicular setting. Another proposal introduced in [5] attempts to predict Doppler changes to allow for easier compensation of the channel effects, the results outperform a benchmark least squares estimation however only simulation results are presented thus its ability to perform under real world constraints are unknown. Further proposals include the use of multiple input multiple output (MIMO) systems [6], cooperative communication [7], and integration into existing long term evolution (LTE) and future 5G systems [8]. There have also been several proposals to use machine learning in the vehicular network, such as in [9] where they investigate the use of artificial neural networks (ANNs) to increase throughput in a vehicular ad-hoc network (VANET) by optimising the medium access control (MAC) layer of the 802.11p protocol. Again, in [10], the use of an online machine learning algorithm is proposed for beam selection in millimetre-wave (mmWave) vehicle-to-anything (V2X) communication to allow network adaptation to traffic and LOS blockages, and the authors in [11] propose machine learning to predict channel state information (CSI). To the best of the authors knowledge at time of writing, there are no attempts at the use of machine learning to equalise and compensate for the vehicular channel.

In this work we will focus on channel compensation using two physical layer waveforms, namely orthogonal frequency division multiplexing (OFDM) and spectrally efficient frequency division multiplexing (SEFDM). The former is the physical layer waveform of choice for the 802.11p standard and is a method commonly deployed in wireless standards due to its robustness against frequency selective fading and relatively simple implementation via the fast Fourier transform (FFT). The available literature on OFDM is vast, spanning decades since its original conception. The latter is a more recent concept first proposed in [12] that utilises the discrete Fourier transform (DFT) to compress the signal in the frequency domain beyond the orthogonality limit of $1/T$, where T is the symbol period. Introducing such a compression improves spectral usage, which is advantageous, but causes self-induced deterministic inter-carrier interference (ICI). As a result of this, over the years, research has been conducted that has resulted in a compression of 30% at reasonable bit-error rates (BERs) using 4-level quadrature amplitude modulation (4-QAM) [13]. The result of the ICI means that complex receivers are required to recover the symbols at the receiver, and to date sphere decoders (SDs) are the most popular choice to take advantage of the newly improved spectral efficiency. In practical implementations, both OFDM and SEFDM require the use of channel state information in conjunction with known pilot symbols as a method of estimating the quality of the channel [14]. This channel estimate can then be used to 'undo' the effects of the channel, before demodulation. In this work, we move away from the typical SD receiver architecture to an artificial neural network (ANN) approach, acting as both a

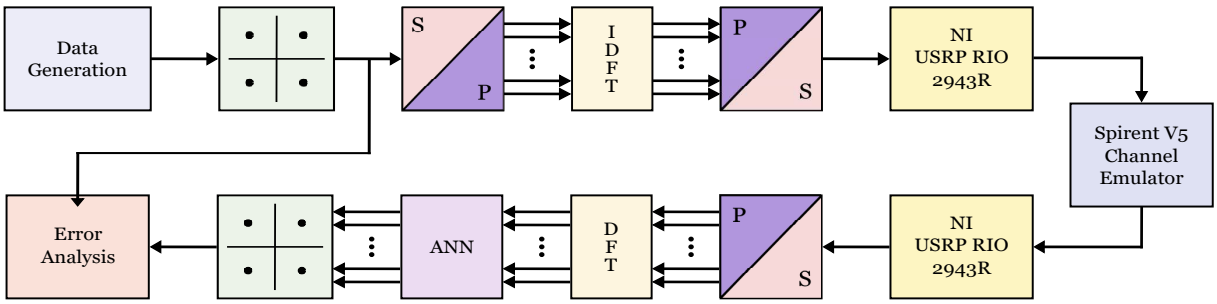

Fig. 1. Block diagram of the test setup

joint channel equaliser and symbol detector. ANNs outperform classic receivers such as decision feedback equalisers and other transversal filters in communications systems [15]. Hence, we propose to utilise the advantages of SEFDM, namely reduced bandwidth and/or higher spectral efficiency, and adopt an ANN as the receiver to increase the performance of vehicular networks. Using SEFDM will advantageously enable the network to either support more users or increase received data rates. For the proposed neural network model, we use a supervised learning approach that does not require CSI. The network is trained on data transmitted over a realistic vehicular channel model to associate received symbols with those transmitted via a known header training sequence. We perform this test via hardware co-simulation, using National Instruments universal software radio peripheral re-configurable input/outputs (NI USRP-RIOs), and a Spirent VR5 channel emulator to generate realistic vehicular channels defined in [16]. We show that by using the neural network OFDM receiver a performance of 4.75 rms error vector magnitude (EVM) over a symbol containing 52 data symbols can be achieved without deviating from the 802.11p standard, however, SEFDM under the same conditions results in a performance of $10.8 \rightarrow 25$ rms EVM as compression factor decreases from $\alpha = 0.8 \rightarrow \alpha = 0.4$.

The rest of the paper is organized as follows. Section II gives some background theory and outlines: in II-A, the experimental test setup for the OFDM and SEFDM transmitters, in II-B, the chosen vehicular channels, and in II-C, the neural network receivers. Section III presents the results, and finally, Section IV gives some concluding remarks.

II. Theory and Experimental Test Setup

A. Transmitter

The experimental test setup is illustrated in Fig. 1. The OFDM and SEFDM signals under test are generated and transmitted using a 'hardware-in-the-loop' approach and the transmitter consists of an NI USRP-RIO 2953R controlled using LabVIEW. First, in each physical frame, $2^{16} - 1$ bits are generated and mapped onto the quadrature phase shift keying (QPSK) constellation. Next, they are passed through a serial-to-parallel converter to be modulated. SEFDM symbols can be constructed with N non-orthogonal subcarriers, and the m^{th} SEFDM symbol's n^{th} subcarrier is modulated by a complex-valued data symbol $s_{m,n}$. The overall discrete-time SEFDM signal $x(t)$ is modulated using a N-point inverse discrete Fourier transform (IDFT), given by [13]:

$$x(t) = \frac{1}{\sqrt{T}} \sum_{m=-\infty}^{\infty} \sum_{n=0}^{N-1} s_{m,n} \exp\left[\frac{j2\pi n\alpha\,(t - mT)}{T}\right] \quad (1)$$

where T is the period of an SEFDM symbol, N is the total number of subcarriers, $s_{m,n}$ is the complex symbol modulated on the n^{th} subcarrier in the m^{th} SEFDM symbol, and $\alpha < 1$ is the bandwidth compression factor, which defines the frequency spacing of the subcarriers. In the OFDM case, $\alpha = 1$ and the subcarrier spacing is set to multiples of $1/T$. A more convenient form for $x(t)$ is in matrix form as follows [13]:

$$X = \mathbf{\Phi} S \quad (2)$$

where X is a P-length vector of the modulated SEFDM symbols in the time-domain, $S = [s_0, s_1 \ldots, s_{N-1}]$ is the input signal in the frequency-domain and $\mathbf{\Phi}$ is an $P \times N$-sized matrix that signifies the sampled carrier matrix [17]. The signals are then serialised and a cyclic prefix of length 25% is added to each symbol before digital-to-analogue conversion.

Considering the carrier matrix $\mathbf{\Phi}$, if $\alpha < 1$, the subcarriers lose orthogonality and overlap, saving bandwidth but causing ICI. The ICI is deterministic and can be modelled as a correlation matrix $\mathbf{C}$ as follows [17]:

$$\mathbf{C}_{(l,n)} = \begin{cases} 1, & l = n \\ \dfrac{1}{N}\left[\dfrac{1 - \exp\left[j2\pi\alpha\,(l-n)\right]}{1 - \exp\left[\frac{j2\pi\alpha(l-n)}{N}\right]}\right], & l \neq n \end{cases} \quad (3)$$

When $\alpha = 1$, $\mathbf{C}$ clearly reduces to an identity matrix $\mathbf{I}$ as expected in the OFDM case. The signals generated follow the 802.11p standard, i.e. the IDFT size is 64, the number of active subcarriers is $N = 52$ and the signal bandwidth was 10 MHz. The particular specifics are documented further in Table I, alongside the values used for α.

B. Vehicular Channel Model

In order to test the proposed system in the most realistic conditions possible, we have opted to use the highway NLOS vehicular channel model presented in [16] and used a Spirent VR5 channel emulator to generate them at 5.9GHz. This channel was chosen as it is the most challenging of the five channel scenarios presented by the authors, having the highest delays, received multipath powers, and doppler shifts. The

TABLE I
TRANSMISSION PARAMETERS

Parameter	Values
Carrier Frequency	5.9GHz
Sampling Frequency	10MSs
Signal Bandwidth	10MHz
Values of α	1 (OFDM), 0.8 : 0.2 : 0.2
FFT/IFFT Size	64 samples
Cyclic Prefix Size	16 samples
Modulation Scheme	QPSK

TABLE II
CHANNEL PARAMETERS

Scenario	Tap	η_i^2 [dB]	τ_i [ns]	$f_{i,d}$ [Hz]	Profile
Highway NLOS	i=1	0	0	0	Static
	i=2	-2	200	689	Half BT
	i=3	-5	433	-492	Half BT
	i=4	-7	700	886	Half BT

main parameters for the channel creation can be found in Table II. All taps are defined as Rayleigh taps with a specified power spectral density (PSD) and a channel bandwidth of 10MHz. This channel model features a half-bathtub shaped Doppler profile which more accurately reflects vehicles communicating in a highway scenario as the dominant contributing scatterers are more densely located directly in front or behind each node [18]. An example PSD can be seen in Fig. 2, along with an empirical cumulative distribution function (ECDF) of the tap realizations in Fig. 3, validating the Rayleigh distribution.

After traversing the signal through the channel using the Spirent VR5 emulator, the signal is then fed to a receiver USRP-RIO 2953R. The received signal considering the vehicular channel H, which is also contaminated by the additive white gaussian noise (AWGN) vector Z may be defined as follows, using (2) [13]:

$$R = \mathbf{\Phi}^* H X + \mathbf{\Phi}^* Z = \mathbf{\Phi}^* H \mathbf{\Phi} S + \mathbf{\Phi}^* Z \tag{4}$$

where R is the demodulated signal vector estimation of X and $(.)^*$ is the Hermitian transpose operation. Thus, clearly aside from the usual considerations not listed mathematically here such as power amplifier non-linearity, the main impediment to successful demodulation of the signals can be identified as H and $\mathbf{C}$.

C. Neural Network Receiver

When the channel is non-static and fading such as the channels used here, finding H and $\mathbf{C}$ becomes highly complex. In general, conventional information theory-based equalisers such as decision feedback or feedforward equalisers are not sufficient to calculate this extremely complex relationship. Thus, due to the advantages of ANNs, such as the ability to generalise any input-output sequence, given sufficient neurons in the hidden layers [19], we select it as the receiver to both calculate H and $\mathbf{C}$.

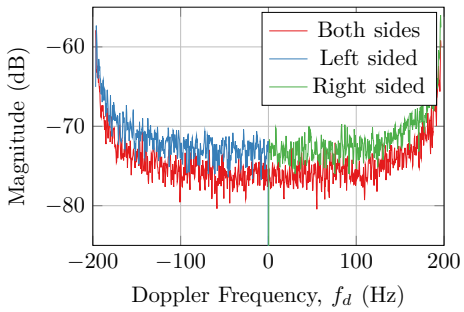

Fig. 2. PSD of an original Jakes trace, with the analytic left and right side PSD examples

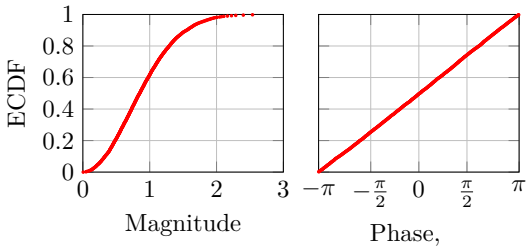

Fig. 3. ECDF of the channels magnitude and phase

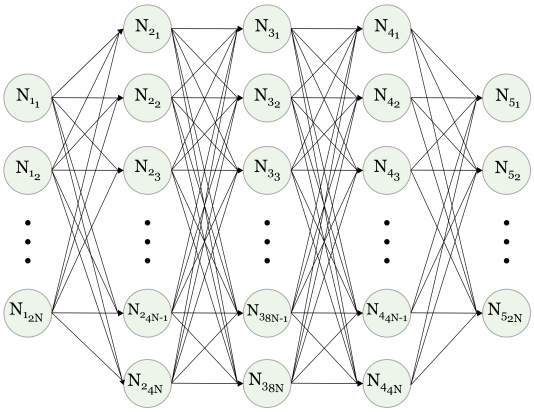

Fig. 4. Block diagram of the neural network

The neural network is designed to be trained on sequences of received QPSK symbols after transmission using either OFDM or SEFDM with a given bandwidth compression factor. A diagram of the model created for this work can be seen in Fig. 4, along with its more in depth parameters in Table III. Since the 802.11p standard defines that 52 subcarriers carry information, the ANN observation vector contains $2N$ neurons, which allows for separation and concatenation of the real and imaginary components of $N = 52$ subcarriers. This allows us to avoid using a split-complex approach which would require two separate ANN models, thus increasing complexity. The network consists of 3 hidden layers with $4N$, $8N$ and $4N$ neurons, as shown in Fig. 4. The reason that 3 hidden layers with this neuron configuration was chosen is inspired from [20] and should be chosen to allow the network enough processing power to capture the complexities of both the channel and the self-induced interference. The received symbols are fed through the network until they reach the output layer, which also contains 104 neurons, mirroring the

input. The 52 real and 52 imaginary outputs are then combined to produce an estimate of original transmitted QPSK symbols.

The optimiser used in this work for the gradient descent algorithm was Nadam [21], a modified version of the Adam gradient descent algorithm that incorporates Nesterov momentum. The advantage of this is that Nesterov momentum has stronger theoretical convergence guarantees for convex functions [22]. The initial learning rate was set to 10^{-3} with a reduction of factor 10^{-1} when the validation loss did not decrease over a 5 epoch period. The loss was evaluated by the common mean square error criterion [23]:

$$L = \frac{1}{2N}\sum_{i=1}^{2N}(y_i - \hat{y}_i)^2 \tag{5}$$

where N in this work would represent the number of subcarriers, $2N$ allows for the separation of the real and imaginary components.

TABLE III
MODEL SUMMARY

Layer	Type	Output Shape	Notes
Input Layer	Input	104	-
Dense	Dense	208	-
Leaky ReLU	Activation	208	$\beta = 0.3$
Dense	Dense	416	-
Leaky ReLU	Activation	416	$\beta = 0.3$
Dense	Dense	208	-
Leaky ReLU	Activation	208	$\beta = 0.3$
Dense	Dense	104	No Bias
Output Later	Output	104	-

III. RESULTS

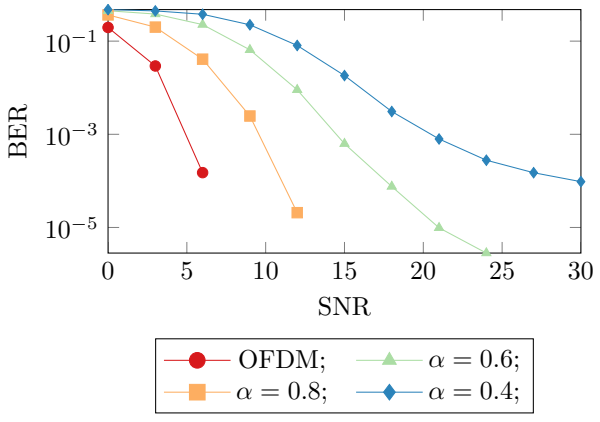

Fig. 5. BER for varying values of α

In this work, we test the performance of OFDM and SEFDM with varying levels of bandwidth compression factor in a realistic 802.11p V2V communication scenario, namely a fast paced urban NLOS scenario. This is done to understand and compare how the effects of a more spectrally efficient waveform may perform if it were introduced as part of the official 802.11p standard versus its baseline counterpart. The bit-error rate (BER) can be seen in Fig. 5, noting however that although they look to have converged, due to the inherent time implications of using of a practical implementation the lesser compressed SEFDM and OFDM cases did not produce any errors beyond 10^{-5}. Due to this, to provide a fair comparison between all the experiments and to inform the reader with the full data, we also measure the EVM of the received constellations with reference to the transmitted constellations. Mathematically, we calculate the EVM as [24]:

$$EVM = \sqrt{\frac{\frac{1}{N}\sum_{k=1}^{N}\left(I_k - \hat{I}_k\right)^2 + \left(Q_k - \hat{Q}_k\right)^2}{\frac{1}{N}\sum_{k=1}^{N}\left(I_k^2 + Q_k^2\right)}} \tag{6}$$

Where I_k and Q_k are the k^{th} original transmitted in-phase and quadrature components respectively, and $\hat{I}_k$ and $\hat{Q}_k$ are the k^{th} observed in-phase and quadrature components respectively.

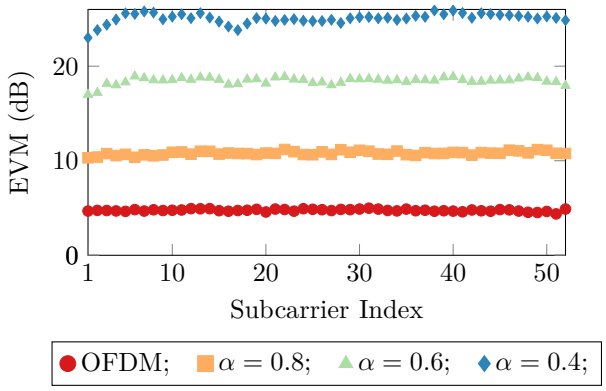

Fig. 6. Error vector magnitude for varying values of α at high SNR

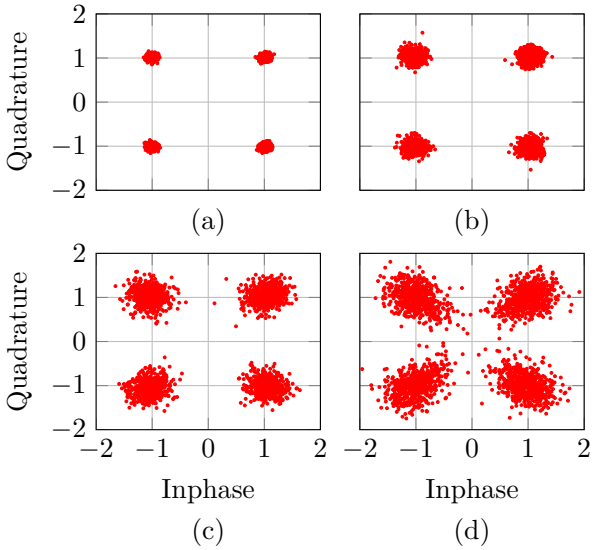

Fig. 7. Received constellations for (a) OFDM, (b) SEFDM with $\alpha = 0.8$, (c) SEFDM with $\alpha = 0.6$ and (d) SEFDM with $\alpha = 0.4$

Fig. 6 illustrates the measured EVM results at high signal-to-noise ratio (SNR) (30dB) for the OFDM system following the defined 802.11p protocol, and the experimental results of

SEFDM with varying bandwidth compression factors. To aid interpretation, representative received constellations for these values can be seen in Fig. 7.

By taking the mean value of the EVM to obtain a single point per SNR (with 95% confidence interval $< 0.1\%$), we observe the trend displayed in Fig. 8. Starting with OFDM, we observe that the EVM decreases sharply until it begins to plateau around 12dB, showing the ANN is quickly able to equalise the channel until the non-deterministic AWGN noise becomes the limiting factor. Turning our attention to SEFDM, with increasing amounts of bandwidth compression we observe the same trend as OFDM, however the limiting factor becomes the combination of the interference caused by the non-orthogonality of the waveform and the non-deterministic AWGN noise.

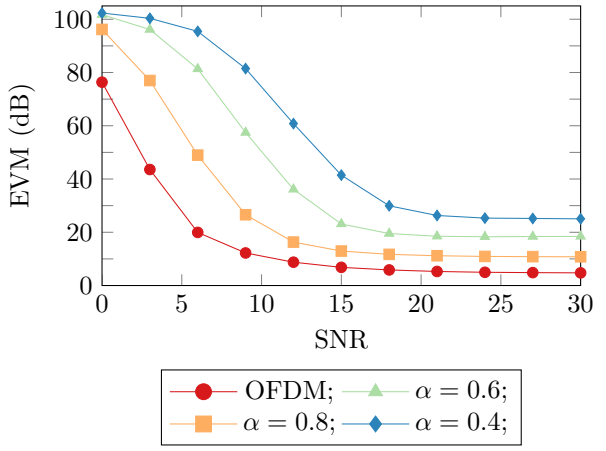

Fig. 8. Mean error vector magnitudes for varying values of α at different SNR's

IV. Conclusion

A neural network receiver has adequate capabilities to be deployed within the vehicular network to adapt and overcome the challenges of the rapidly changing environment. Practical experiments were undertaken using a hardware-in-the-loop approach which demonstrated the efficacy of the proposed method, both conforming to the current 802.11p standard using OFDM and with the more spectrally efficient waveform SEFDM. SEFDM is tested with compression factors ranging from 20% up to 60% bandwidth compression, these spectral savings could be used in future to improve data rates or service more users. The results have demonstrated that an acceptable BER performance can be achieved under the harsh conditions of a highway NLOS vehicular channel. This was further validated via measurements of the error vector magnitude.

V. Acknowledgement

Scott Stainton acknowledges an EPSRC studentship for his PhD studies. Waseem Ozan acknowledges a UCL studentship for his PhD studies. The authors would like to acknowledge Prof. Izzat Darwazeh at UCL for enabling the experimentation through access to the channel emulator. This paper was funded by the EPSRC grant EP/P006280/1 MARVEL.

References

[1] H. Boeglen *et al.*, "A survey of V2V channel modeling for VANET simulations," in *8th WONS 2011*. IEEE, jan 2011, pp. 117–123.

[2] A. F. Molisch *et al.*, "A survey on vehicle-to-vehicle propagation channels," *IEEE Wireless Communications*, vol. 16, no. 6, pp. 12–22, 2009.

[3] C. F. Mecklenbraüker *et al.*, "Vehicular channel characterization and its implications for wireless system design and performance," *Proceedings of the IEEE*, vol. 99, no. 7, pp. 1189–1212, 2011.

[4] Y. Kaymak *et al.*, "Indirect Diffused Light Free-Space Optical Communications for Vehicular Networks," *IEEE Communications Letters*, vol. 23, no. 5, pp. 814–817, may 2019.

[5] R. Alieiev *et al.*, "Predictive Communication and Its Application to Vehicular Environments: Doppler-Shift Compensation," *IEEE Transactions on Vehicular Technology*, vol. 67, no. 8, pp. 7380–7393, aug 2018.

[6] T. Izydorczyk *et al.*, "Performance evaluation of multi-antenna receivers for vehicular communications in live LTE networks," in *IEEE Vehicular Technology Conference*, vol. 2019-April. Institute of Electrical and Electronics Engineers Inc., apr 2019.

[7] E. Ahmed *et al.*, "Cooperative Vehicular Networking: A Survey," *IEEE Transactions on Intelligent Transportation Systems*, vol. 19, no. 3, pp. 996–1014, mar 2018.

[8] S. A. A. Shah *et al.*, "5G for Vehicular Communications," *IEEE Communications Magazine*, vol. 56, no. 1, pp. 111–117, jan 2018.

[9] M. A. Karabulut *et al.*, "Performance optimization by using artificial neural network algorithms in vanets," in *42nd TSP 2019*. IEEE, 2019, pp. 633–636.

[10] G. H. Sim *et al.*, "An online context-aware machine learning algorithm for 5g mmwave vehicular communications," *IEEE/ACM Transactions on Networking*, vol. 26, no. 6, pp. 2487–2500, dec 2018.

[11] J. Joo *et al.*, "Deep Learning-Based Channel Prediction in Realistic Vehicular Communications," *IEEE Access*, vol. 7, pp. 27 846–27 858, 2019.

[12] M. R. D. Rodrigues *et al.*, "A spectrally efficient frequency division based communications system," *ISBC 2006*, no. September, 2006.

[13] W. Ozan *et al.*, "Experimental SEFDM Pipelined Iterative Detection Architecture with Improved Throughput," in *VTC 2018*, vol. 2018-June. Institute of Electrical and Electronics Engineers Inc., jul 2018, pp. 1–5.

[14] W. Ozan *et al.*, "Experimental evaluation of channel estimation and equalisation in non-orthogonal fdm systems," in *11th CSNDSP 2018*, July 2018, pp. 1–6.

[15] K. Burse *et al.*, "Channel equalization using neural networks: A review," *IEEE transactions on systems, man, and cybernetics, Part C (Applications and Reviews)*, vol. 40, no. 3, pp. 352–357, 2010.

[16] T. Blazek *et al.*, "Vehicular channel models: A system level performance analysis of tapped delay line models," in *15th ITST 2017*. IEEE, may 2017, pp. 1–8.

[17] W. Ozan *et al.*, "Time precoding enabled Non-Orthogonal frequency division multiplexing," Istanbul, Turkey, sep 2019.

[18] A. Paier *et al.*, "Overview of vehicle-to-vehicle radio channel measurements for collision avoidance applications," *VTC 2010*, pp. 4–8, 2010.

[19] A. Zerguine *et al.*, "Multilayer perceptron-based dfe with lattice structure," *IEEE transactions on neural networks*, vol. 12, no. 3, pp. 532–545, 2001.

[20] H. Ye *et al.*, "Power of Deep Learning for Channel Estimation and Signal Detection in OFDM Systems," *IEEE Wireless Communications Letters*, vol. 7, no. 1, pp. 114–117, feb 2018.

[21] T. Dozat, "Incorporating Nesterov Momentum into Adam," *ICLR Workshop*, no. 1, pp. 2013–2016, 2016.

[22] I. Sutskever *et al.*, "On the importance of initialization and momentum in deep learning," in *30th ICML 2013*, no. PART 3, 2013, pp. 2176–2184.

[23] W. Schmidt *et al.*, "Initializations, back-propagation and generalization of feed-forward classifiers," in *IEEE International Conference on Neural Networks*. IEEE, pp. 598–604.

[24] S. T. Le *et al.*, "Comparison of numerical bit error rate estimation methods in 112Gbs QPSK CO-OFDM transmission," in *IET Conference Publications*, vol. 2013, no. 622 CP, 2013, pp. 1083–1085.